ACS Macro Letters

Letter

pubs.acs.org/macroletters

A Four-Arm Star-Shaped Poly(ethylene glycol) (StarPEG) Platform for Bombesin Peptide Delivery to Gastrin-Releasing Peptide Receptors in Prostate Cancer

Yingding Xu,[†,∥] Wei Huang,[‡,∥] Gang Ren,[†,∥] Shibo Qi,[†] Han Jiang,[†] Zheng Miao,[†] Hongguang Liu,[†] Ermelinda Lucente,[†] Lihong Bu,[†,§] Baozhong Shen,[§] Annelise Barron,[‡] and Zhen Cheng*[,†]

[†]Molecular Imaging Program at Stanford (MIPS), Department of Radiology and Bio-X Program, Canary Center at Stanford for Cancer Early Detection, Stanford University, Stanford, California, 94305-5344, United States

[‡]Department of Bioengineering, Stanford University, Stanford, California 94305-5344, United States

[§]Department of Radiology, Fourth Affiliated Hospital of Harbin Medical University, Harbin, China 150001

ABSTRACT: We present the design, synthesis, and characterization of a novel cancer biomarker delivery platform, the star-shaped four-arm poly(ethylene glycol) (StarPEG). Using the multidisplay platform we were able to synthesize a bombesin (BBN) positron emission tomography (PET) probe featuring four copies of 8-Aoc-BBN peptides (where 8-Aoc is 8-aminooctanic acid), which we named StarPEG-BBN. Cell binding studies showed that StarPEG-BBN had a good binding affinity to PC3 cells (IC_{50} = 65.3 ± 3.4 nM). Cell uptake studies showed that the binding was specific (blocking vs no-blocking, $P < 0.05$). Mice were then implanted with PC3 cells and divided into two groups, one injected with ^{64}Cu-StarPEG-BBN and the other 250 μg of unlabeled 8-Aoc-BBN along with ^{64}Cu-StarPEG-BBN. In vivo images revealed that StarPEG-BBN had good tumor uptake (4.2 ± 0.4% ID/g at 4 h post-injection (p.i.)) and was significantly blocked by coinjection of unlabeled 8-Aoc-BBN at 4 h p.i. ($P = 0.003$). The small animal PET quantification was further verified by the biodistribution study at 24 h p.i. Our study demonstrated that the novel four-arm PEG platform StarPEG as a cancer biomarker multimerization/delivery platform conserves binding specificity, improves drug loading, is capable of achieving good tumor uptake, and has great potential in cancer treatment and molecular imaging.

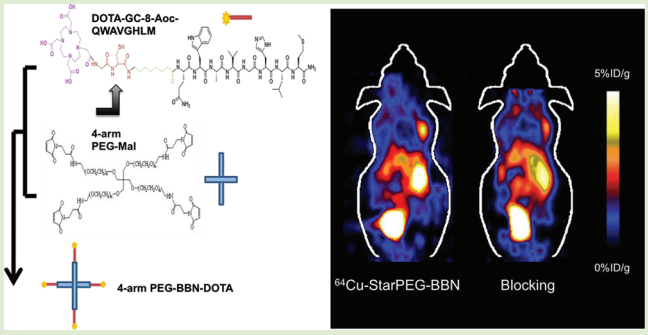

In recent years, macromolecules such as nanoscale soluble polymers, dendrimers, liposomes, and others have been increasingly used as drug delivery systems (DDS) for anticancer therapies.[1−3] Many of the carriers that have been developed are able to achieve specific targeting via two principal mechanisms. Passive targeting allows specificity on the tissue level, while the capability of conjugation with biological ligands such as peptides permits targeting on the molecular level. With these unique properties macromolecule-based DDS have been proven to be superior to the conventional therapeutics.

On the other hand, low molecular weight anticancer agents generally suffer from fast clearance from the blood circulation and thus a relatively low tumor uptake and short tumor retention for in vivo application.[4,5] PEGylation (PEG: poly(ethylene glycol)) has been extensively used to prolong the half-life of small peptides or drugs and enhance their stability and bioavailability in the plasma.[6−10] This general chemical modification strategy also improves accumulation in tumor tissues over time via the enhanced permeability and retention (EPR) effect, which provides passive tumor targeting.[4,11] For instance, an anticancer DDS with PEG (MW ≈ 5000) as the linker connecting apoptosis-inducing agent camptothecin (CPT) and luteinizing-hormone-releasing hormone (LHRH) peptides as the targeting moiety (LHRH-PEG-CPT) was found to have significantly enhanced therapeutic efficacy when compared to CPT or CPT-PEG.[12]

However, using PEG as the carrier for low molecular weight anticancer drugs also has major caveats particularly regarding clinical feasibility. The major limitations here are two-fold, including low targeting specificity and suboptimal drug loading capability. To counter the first limitation targeted anticancer conjugates using peptides, antibodies, hormones, and other small molecules have been widely investigated.[13] To counter the second and the more difficult limitation, multimerization via multiple-arm PEG can be envisioned to be helpful since this strategy can significantly increase the targeting moiety/polymer ratio. Of note, multiple-arm PEG structures such as the well-developed four-arm PEG also provide an intrinsic spatial separation among targeting residues and thus maximizes

Received: March 6, 2012
Accepted: May 30, 2012
Published: June 4, 2012

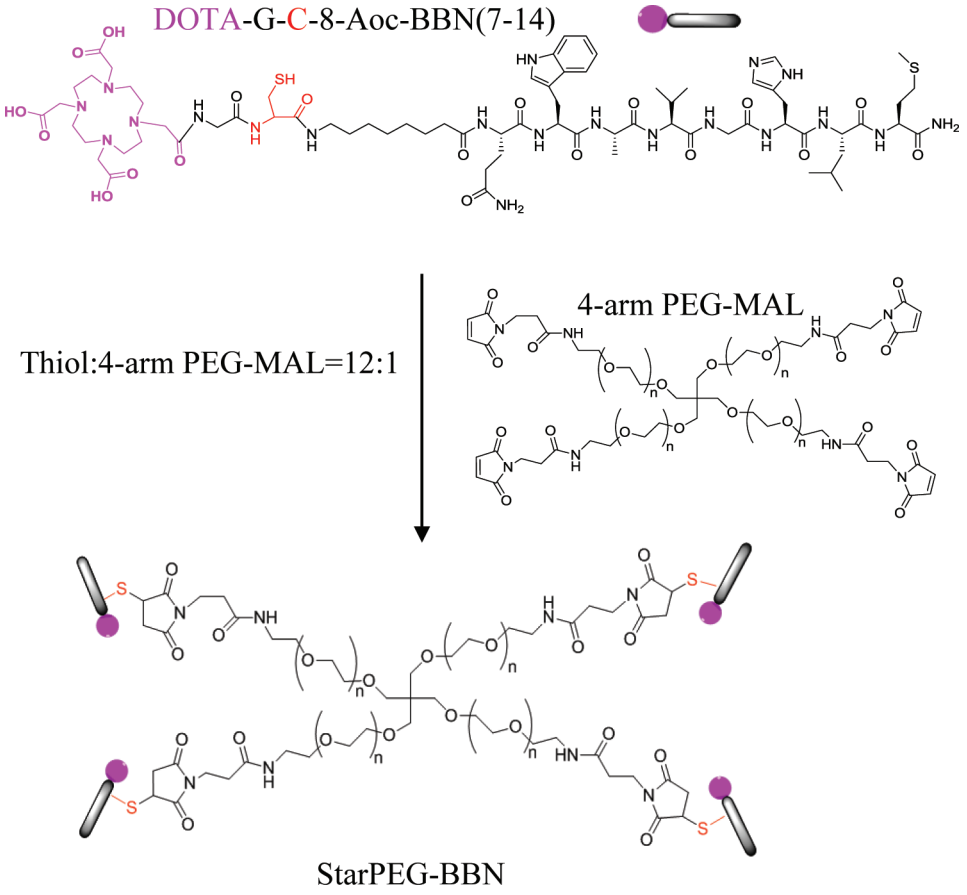

Figure 1. Chemical structures of DOTA-G-C-8-Aoc-BBN(7−14) and the four-arm PEG-MAL and an illustration of the synthesis of StarPEG-BBN conjugates. Peptides and the four-arm PEG-MAL were dissolved in PBS, pH 7.4 at 10 mg/mL, and they were mixed together to make the ratio of 12 mol of thiols to 1 mol of four-arm PEG-MAL.

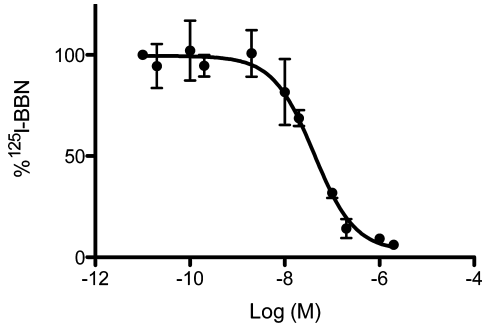

Figure 2. Binding affinity assay of StarPEG-BBN (n = 4, mean ± SD). IC_{50} was measured to be 65.3 ± 3.4 nM.

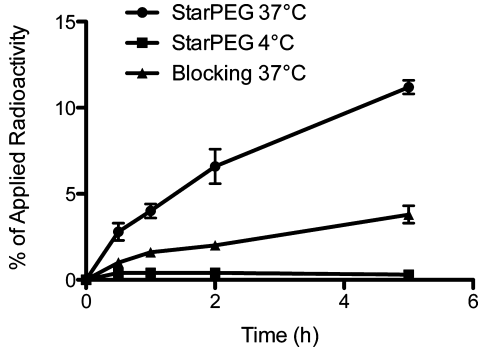

Figure 3. Cellular uptake studies of ^{64}Cu-StarPEG-BBN at 37 and 4 °C and ^{64}Cu-StarPEG-BBN blocked by unlabeled 8-Aoc-BBN at 37 °C in PC3 cell line (n = 3, mean ± SD).

specific targeting and potentially enhances simultaneous binding by avoiding steric hindrance.

In recent years, four-arm PEG molecules have seen applications in hydrogels, biotinylation, hypoglycemic agent half-life prolongation, and nanoparticle surface modification.[14−20] However, it has never been exploited as a DDS for bioactive molecules for tumor targeting. We hypothesized that four-arm PEG structures can act as a very effective platform for small peptide delivery and even molecular imaging because they not only provide the intrinsic characteristics of monomer PEG such as prolonged retention, increased hydrophilicity, and enhanced stability, but also the advantages unique to multiple-arm PEG such as improved drug loading, maximized specific targeting, and the potential benefit of simultaneous binding.

Bombesin (BBN) peptides can bind with high affinity and specificity to gastrin-releasing peptide receptors (GRPR), which are up-regulated in various types of cancers including prostate cancer, and thus has been regarded as an important biomarker for malignant transformation.[21,22] In prostate cancer, it was reported the high expression of GRPR in 30 of the 30 tested invasive prostatic carcinoma.[23] Hence, BBN peptides provide a promising basis for developing diagnostic or therapeutic agents to target GRPR positive prostate cancers.[21,22,24] Herein, we report a design of a StarPEG platform conjugated with multivalent BBN(7−14) (Q-W-A-V-G-H-L-M) peptide for targeted delivery to the GRPR positive prostate cancer. We

dx.doi.org/10.1021/mz300105n | ACS Macro Lett. 2012, 1, 753−757

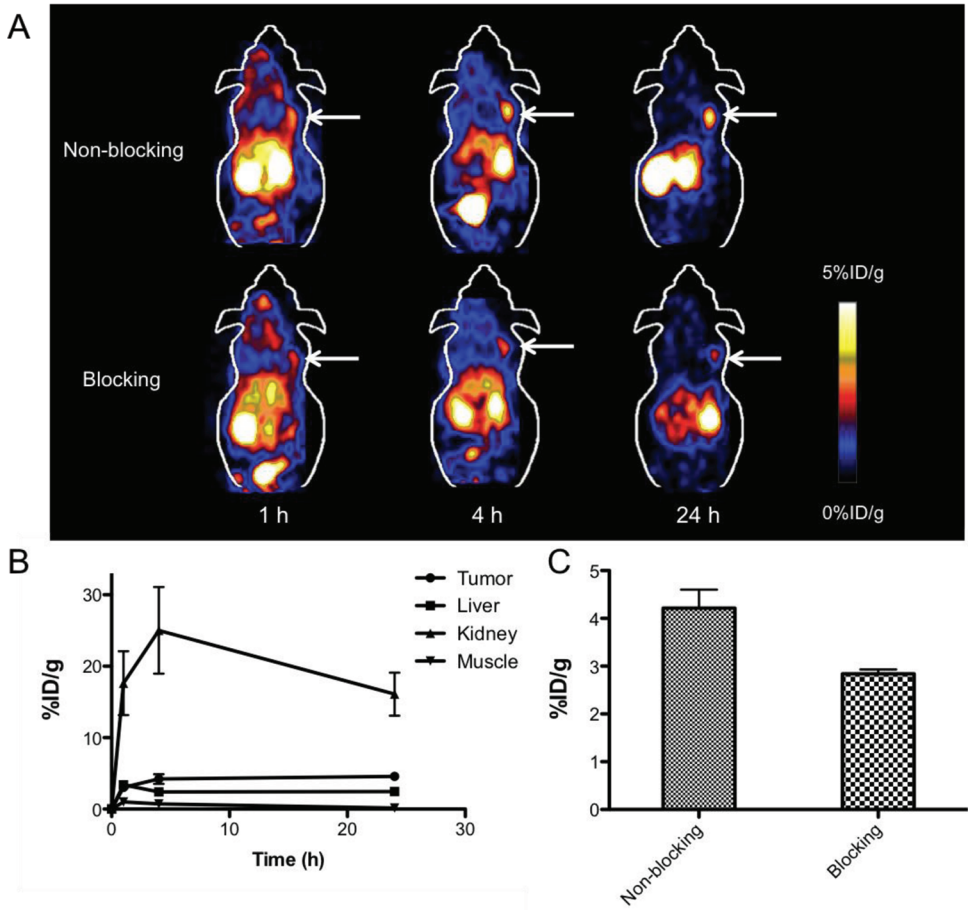

Figure 4. (A) In vivo imaging in PC3 murine models. Top row from left to right: representative PET images of PC3 tumor mice injected with ^{64}Cu-StarPEG-BBN at 1, 4, and 24 h p.i.; bottom row from left to right: representative PET images of PC3 tumor mice injected with both ^{64}Cu-StarPEG-BBN and 250 μg of unlabeled 8-Aoc-BBN at 1, 4, and 24 h p.i. (B) Small animal PET quantification of tumor, liver, kidney, and muscle of PC3 tumor mice injected with ^{64}Cu-StarPEG-BBN at 1, 4, and 24 h p.i. (C) Small animal PET quantification of tumor uptake of PC3 tumor mice injected with ^{64}Cu-StarPEG-BBN alone compared with PC3 tumor mice injected with both ^{64}Cu-StarPEG-BBN and 250 μg of unlabeled 8-Aoc-BBN at 4 h p.i.

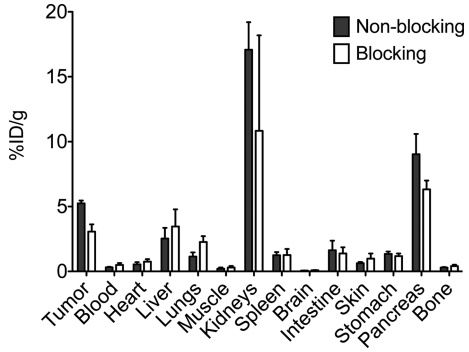

Figure 5. Biodistribution studies of ^{64}Cu-StarPEG-BBN and ^{64}Cu-StarPEG-BBN blocked by unlabeled 8-Aoc-BBN in PC3 tumor-bearing athymic nude mice at 24 h p.i. Tumor uptakes for ^{64}Cu-StarPEG-BBN and ^{64}Cu-StarPEG-BBN with unlabeled 8-Aoc-BBN were 5.3 ± 0.2% ID/g and 3.1 ± 0.6% ID/g, respectively, P = 0.003. Data are expressed as a normalized accumulation of activity in % ID/g ± SD (n = 3).

envisioned this research to be a proof-of-principle study demonstrating the efficacy of StarPEG as a novel DDS and an imaging platform for low molecular weight biomolecules.

The four-arm PEG-maleimide with a molecular weight (MW) of ∼10 KDa was used as the carrier to multidisplay BBN peptides. The PEG's MW was chosen for safety concerns given kidney's excretion limits of large molecules.[25] The thiol-maleimide chemistry was adopted for a specific and easy peptide-PEG conjugation. The 8-aminooctanoic acid (8-Aoc) has been reported as an effective spacer between the labeling moiety and the BBN peptide with the ease of synthesis.[22,26] A cysteine residue was further designed in the spacer part to provide a thiol for further coupling with the maleimide groups presented in StarPEG. A 1,4,7,10-tetraazacyclododecane-1,4,7,10-tetraacetic acid (DOTA) chelator was also added for labeling with radionculides such as the positron emitter ^{64}Cu ($t_{1/2}$ = 12.7 h, $E_{\beta^+\,max}$ = 656 keV, 19%) for imaging purposes. Taken together, the four-arm PEG-MAL and DOTA-G-C-8-Aoc-BBN(7−14) were designed to synthesize a StarPEG-based platform with multivalent BBN peptides for prostate cancer targeting (Figure 1). Purified DOTA-G-C-8-Aoc-BBN(7−14) reacted with the four-arm PEG-MAL with a thiol-to-maleimide ratio at 3:1 (12 mol of thiols to 1 mol of four-arm PEG-MAL), and the StarPEG-BBN conjugates were further purified with RP-HPLC. By analyzing the molecular weight of the resulting conjugates via matrix-assisted laser desorption/ionization time-of-flight mass spectrometry (MALDI-TOF-MS), the functionalizing ratio of BBN to StarPEG is ∼4, with the four arms of each PEG all functionalized with BBN peptides.

dx.doi.org/10.1021/mz300105n | ACS Macro Lett. 2012, 1, 753−757

The competitive cell-binding assay was used to determine the receptor-binding affinity of StarPEG-BBN. StarPEG-BBN inhibited the binding of ^{125}I-[Tyr4]BBN to PC3 cells in a concentration-dependent manner (Figure 2). The IC_{50} value of StarPEG-BBN was determined to be 65.3 ± 3.4 nM. This IC_{50} value suggests that the conjugation of the BBN peptides to the four-arm PEG results in a reasonable binding affinity to GRPR in vitro and StarPEG-BBN can be used for further in vivo evaluation. StarPEG-BBN conjugate was then successfully labeled with ^{64}Cu at 50 °C for 1 h of incubation. The purification of radiolabeling solution using reversed phase high-performance liquid chromatography (RP-HPLC) afforded ^{64}Cu-StarPEG-BBN with >95% radiochemical purity and a modest specific activity of 40 μCi/μg as determined by analytic HPLC (decay corrected). The cell uptake studies of ^{64}Cu-StarPEG-BBN with and without blocking were performed on PC3 cells. As shown in Figure 3, the radiolabeled macromolecules exhibited an increased uptake with time. Generally speaking, most of the ^{64}Cu-StarPEG-BBNs were internalized at 37 °C as evidenced by the difference in cellular uptake of applied radioactivity from 4 °C, at which temperature cellular internalization is mostly suppressed. Comparing the blocking and nonblocking groups of the study, the uptake of ^{64}Cu-StarPEG-BBN was significantly lower when the cells were incubated with unlabeled 8-Aoc-BBN peptide at all time points ($P < 0.05$), indicating the specificity of binding and uptake of the labeled molecule.

Animal procedures were performed according to a protocol approved by Stanford University. For small animal positron emission tomography (PET) studies, nude mice were implanted with PC3 cells in the right shoulder and divided into two groups ($n = 3$ each). The first group was injected with about 3.7 MBq (100 μCi) of ^{64}Cu-StarPEG-BBN; the second group was injected with 250 μg of unlabeled 8-Aoc-BBN along with 3.7 MBq of ^{64}Cu-StarPEG-BBN. Mice were then imaged with PET at 1, 4, and 24 h post injection (p.i.). Representative decay-corrected coronal images are shown in Figure 4A. The PC3 tumors were clearly visualized with good tumor-to-background contrast for ^{64}Cu-StarPEG-BBN, and tumor uptake was quantified to be 3.0 ± 0.2%, 4.2 ± 0.7%, and 4.6 ± 0.6% of the injected radioactive dose per gram of tissue (% ID/g) at 1 h, 4 h, and 24 h p.i., respectively (values expressed in mean ± standard deviation (SD), $n = 3$, Figure 4B). Quantification across tumor, liver, kidneys, and muscle gave further insights into the pharmacokinetics of StarPEG-BBN (Figure 4B). The vast majority of the radiolabeled molecules was clearly excreted through the kidneys. Tumor uptake quickly plateaued at 4 h p.i. and maintained at peak levels at 24 h p.i. Liver uptake was much lower than that of kidneys, and muscle uptake was minimal. Figure 4A also revealed that ^{64}Cu-StarPEG-BBN was significantly blocked by coinjection of unlabeled 8-Aoc-BBN, particularly at 4 and 24 h p.i. This finding confirms specific targeting of ^{64}Cu-StarPEG-BBN in the GRPR-positive PC3 tumor. To further verify specificity of StarPEG-BBN quantification yielded tumor uptakes of 2.6 ± 0.5% ID/g, 2.8 ± 0.2% ID/g, and 2.8 ± 0.1% ID/g at 1 h, 4 h, and 24 h p.i., respectively, when blocked by unlabeled BBN monomer (values expressed in mean ± SD, $n = 3$). A direct visual comparison of tumor uptake values at 4 h p.i. is shown in Figure 4C ($P < 0.05$).

For biodistribution studies, mice bearing PC3 xenografts ($n = 3$) were injected with about 3.7 MBq (100 μCi) of ^{64}Cu-StarPEG-BBN and sacrificed at 24 h p.i. Blocking was achieved by coinjection of the probe with 250 μg of unlabeled 8-Aoc-BBN. The tumor and normal organs of interest were removed and weighed, and their radioactivity was measured in a gamma-counter. The results are shown in Figure 5. The tumor uptake for ^{64}Cu-StarPEG-BBN with and without unlabeled Aoc-BBN was 3.1 ± 0.6% ID/g and 5.3 ± 0.2% ID/g, respectively ($P = 0.003$). Liver and kidney uptakes were not statistically significant comparing the blocked and the nonblocked radiotracers. However, a significant blocking effect was observed in pancreas ($P < 0.05$), which is consistent with the fact that murine pancreatic cells express a very high level of GRPR.

In conclusion, StarPEG can be used as a novel and efficient platform for multimerization/delivery of cancer targeting molecules for in vivo applications. It conserves binding specificity, improves drug loading, is able to achieve good imaging contrast, and has great potential in cancer treatment and molecular imaging.

AUTHOR INFORMATION

Corresponding Author

*Address: Molecular Imaging Program at Stanford Department of Radiology and Bio-X Program, Canary Center at Stanford for Cancer Early Detection, 1201 Welch Road, Lucas Expansion P095, Stanford University, Stanford, CA 94305. Phone: 650-723-7866. Fax: 650-736-7925. E-mail: zcheng@stanford.edu.

Author Contributions

‖These authors contributed to this work equally.

Notes

The authors declare no competing financial interest.

ACKNOWLEDGMENTS

We acknowledge the support from the DOD-PCRP-NIA PC094646 (ZC), Stanford Medical Scholar Research Fellowship (YX), the international cooperation projects of the Chinese Ministry of Science and Technology (2009DFB30040), the National Science Foundation for Postdoctoral Scientists of China (20070420165), and the Science and Technology Tackle Key Problem Plan Foundation of Harbin (2007AA3CS085).

REFERENCES

(1) Nori, A.; Kopecek, J. *Adv. Drug Delivery Rev.* **2005**, *57* (4), 609–36.

(2) Onishi, H.; Machida, Y. *Molecules* **2008**, *13* (9), 2136–55.

(3) Khare, P.; Jain, A.; Gulbake, A.; Soni, V.; Jain, N. K.; Jain, S. K. *Crit. Rev. Ther. Drug Carrier Syst.* **2009**, *26* (2), 119–55.

(4) Allen, T. M.; Cullis, P. R. *Science* **2004**, *303* (5665), 1818–1822.

(5) Zhang, X.; Cai, W.; Cao, F.; Schreibmann, E.; Wu, Y.; Wu, J. C.; Xing, L.; Chen, X. *J. Nucl. Med.* **2006**, *47* (3), 492–501.

(6) Veronese, F. M. *Biomaterials* **2001**, *22* (5), 405–17.

(7) Harris, J. M.; Chess, R. B. *Nat. Rev. Drug Discovery* **2003**, *2* (3), 214–21.

(8) Jevsevar, S.; Kunstelj, M.; Porekar, V. G. *Biotechnol. J.* **2010**, *5* (1), 113–28.

(9) Jokerst, J. V.; Lobovkina, T.; Zare, R. N.; Gambhir, S. S. *Nanomedicine (London)* **2011**, *6* (4), 715–28.

(10) Pasut, G.; Veronese, F. M. *J. Controlled Release* **2011**, PMID: 22094104.

(11) Iyer, A. K.; Khaled, G.; Fang, J.; Maeda, H. *Drug Discovery Today* **2006**, *11* (17–18), 812–818.

(12) Dharap, S. S.; Wang, Y.; Chandna, P.; Khandare, J. J.; Qiu, B.; Gunaseelan, S.; Sinko, P. J.; Stein, S.; Farmanfarmaian, A.; Minko, T. *Proc. Natl. Acad. Sci. U.S.A.* **2005**, *102* (36), 12962–7.

(13) Allen, T. M. *Nat. Rev. Cancer* **2002**, *2* (10), 750−63.
(14) Browning, M. B.; Wilems, T.; Hahn, M.; Cosgriff-Hernandez, E. *J. Biomed. Mater. Res., Part A* **2011**, *98* (2), 268−73.
(15) Ding, H.; Yong, K. T.; Roy, I.; Hu, R.; Wu, F.; Zhao, L.; Law, W. C.; Zhao, W.; Ji, W.; Liu, L.; Bergey, E. J.; Prasad, P. N. *Nanotechnology* **2011**, *22* (16), 165101.
(16) Iwasaki, Y.; Ota, T. *Chem. Commun. (Cambridge, U.K.)* **2011**, *47* (37), 10329−31.
(17) Jeong, S. Y.; Hwang, M. H.; Kim, J. E.; Kang, S.; Park, J. C.; Yoo, J.; Ha, J. H.; Lee, S. W.; Ahn, B. C.; Lee, J. *Endocr. J.* **2011**, *58* (7), 575−83.
(18) Liu, Z.; Yan, Y.; Chin, F. T.; Wang, F.; Chen, X. *J. Med. Chem.* **2009**, *52* (2), 425−32.
(19) Shikanov, A.; Smith, R. M.; Xu, M.; Woodruff, T. K.; Shea, L. D. *Biomaterials* **2011**, *32* (10), 2524−31.
(20) Yang, J.; Jacobsen, M. T.; Pan, H.; Kopecek, J. *Macromol. Biosci.* **2010**, *10* (4), 445−54.
(21) Chanda, N.; Kattumuri, V.; Shukla, R.; Zambre, A.; Katti, K.; Upendran, A.; Kulkarni, R. R.; Kan, P.; Fent, G. M.; Casteel, S. W.; Smith, C. J.; Boote, E.; Robertson, J. D.; Cutler, C.; Lever, J. R.; Katti, K. V.; Kannan, R. *Proc. Natl. Acad. Sci. U.S.A.* **2010**, *107* (19), 8760−8765.
(22) Prasanphanich, A. F.; Nanda, P. K.; Rold, T. L.; Ma, L. X.; Lewis, M. R.; Garrison, J. C.; Hoffman, T. J.; Sieckman, G. L.; Figueroa, S. D.; Smith, C. J. *Proc. Natl. Acad. Sci. U.S.A.* **2007**, *104* (30), 12462−12467.
(23) Markwalder, R.; Reubi, J. C. *Cancer Res.* **1999**, *59* (5), 1152−1159.
(24) Lantry, L. E.; Cappelletti, E.; Maddalena, M. E.; Fox, J. S.; Feng, W. W.; Chen, J. Q.; Thomas, R.; Eaton, S. M.; Bogdan, N. J.; Arunachalam, T.; Reubi, J. C.; Raju, N.; Metcalfe, E. C.; Lattuada, L.; Linder, K. E.; Swenson, R. E.; Tweedle, M. F.; Nunn, A. D. *J. Nucl. Med.* **2006**, *47* (7), 1144−1152.
(25) Veronese, F. M.; Pasut, G. *Drug Discovery Today* **2005**, *10* (21), 1451−8.
(26) Garrison, J. C.; Rold, T. L.; Sieckman, G. L.; Naz, F.; Sublett, S. V.; Figueroa, S. D.; Volkert, W. A.; Hoffman, T. J. *Bioconjugate Chem.* **2008**, *19* (9), 1803−1812.